JAM-A associates with ZO-2, afadin, and PDZ-GEF1 to activate Rap2c and regulate epithelial barrier function

Ana C. Monteiro[a], Ronen Sumagin[a], Carl R. Rankin[a], Giovanna Leoni[a], Michael J. Mina[b], Dirk M. Reiter[c], Thilo Stehle[c,d], Terence S. Dermody[d,e,f], Stacy A. Schaefer[g], Randy A. Hall[g], Asma Nusrat[a], and Charles A. Parkos[a]

[a]Department of Pathology and [g]Department of Pharmacology, Emory University School of Medicine, Atlanta, GA 30306; [b]Emory Rollins School of Public Health, Atlanta, GA 30306; [c]Interfaculty Institute of Biochemistry, University of Tübingen, D-72076 Tübingen, Germany; [d]Department of Pediatrics and Pathology, [e]Departments of Microbiology and Immunology, and [f]Elizabeth B. Lamb Center for Pediatric Research, Vanderbilt University School of Medicine, Nashville, TN 37230

ABSTRACT **Intestinal barrier function is regulated by epithelial tight junctions (TJs), structures that control paracellular permeability. Junctional adhesion molecule-A (JAM-A) is a TJ-associated protein that regulates barrier; however, mechanisms linking JAM-A to epithelial permeability are poorly understood. Here we report that JAM-A associates directly with ZO-2 and indirectly with afadin, and this complex, along with PDZ-GEF1, activates the small GTPase Rap2c. Supporting a functional link, small interfering RNA–mediated down-regulation of the foregoing regulatory proteins results in enhanced permeability similar to that observed after JAM-A loss. JAM-A–deficient mice and cultured epithelial cells demonstrate enhanced paracellular permeability to large molecules, revealing a potential role of JAM-A in controlling perijunctional actin cytoskeleton in addition to its previously reported role in regulating claudin proteins and small-molecule permeability. Further experiments suggest that JAM-A does not regulate actin turnover but modulates activity of RhoA and phosphorylation of nonmuscle myosin, both implicated in actomyosin contraction. These results suggest that JAM-A regulates epithelial permeability via association with ZO-2, afadin, and PDZ-GEF1 to activate Rap2c and control contraction of the apical cytoskeleton.**

Monitoring Editor
Keith E. Mostov
University of California, San Francisco

Received: Jun 3, 2013
Revised: Jul 11, 2013
Accepted: Jul 12, 2013

INTRODUCTION

The colonic epithelium facilitates selective absorption of nutrients while precluding the passage of toxins and pathogens into the body. This selective permeability is regulated by tight junctions (TJs), which are complex, dynamic structures that localize to the apical contacts between epithelial cells. It is well appreciated that TJs are composed of a diverse array of structural and signaling proteins, including junctional adhesion molecule-A (JAM-A). JAM-A is a transmembrane protein constituent of TJs that regulates epithelial barrier function in addition to other homeostatic properties such as epithelial cell migration and proliferation (Laukoetter *et al.*, 2007; Severson *et al.*, 2008; Nava *et al.*, 2011).

There are several reports linking JAM-A to regulation of epithelial barrier function. For example, JAM-A–knockout mice have enhanced colonic permeability, and epithelial cells lacking JAM-A have decreased transepithelial electrical resistance (TER) and enhanced paracellular flux of low–molecular weight dextran in vitro (Laukoetter *et al.*, 2007). Previous studies linking JAM-A structure to cellular function indicated that JAM-A forms homodimers on the surface of the same cell (in-*cis*) at its membrane-distal immunoglobulin domain (Kostrewa *et al.*, 2001; Prota *et al.*, 2003) and that *cis*-dimerization is required for epithelial cell migration and barrier function (Liu *et al.*,

This article was published online ahead of print in MBoC in Press (http://www.molbiolcell.org/cgi/doi/10.1091/mbc.E13-06-0298) on July 24, 2013.

Address correspondence to: Charles Parkos (cparkos@emory.edu).

The authors declare no conflict of interest.

Abbreviations used: AJC, apical junctional complex; FRAP, fluorescence recovery after photobleaching; GST, glutathione *S*-transferase; IEC, intestinal epithelial cells; JAM-A, junctional adhesion molecule-A; MLC, myosin light chain; PDZ, postsynaptic density protein, *Drosophila* disc large tumor repressor, zonula occludens-1; PDZ-GEF1/2, PDZ guanine exchange factor 1/2; TJ, tight junction; ZO-1/2, zonula occludens-1/2.

Supplemental Material can be found at:
http://www.molbiolcell.org/content/suppl/2013/07/22/mbc.E13-06-0298.DC1.html

2000; Mandell *et al.*, 2004; Severson *et al.*, 2008). JAM-A was reported to associate with signaling molecules such as the scaffold proteins ZO-1 and afadin, as well as with the guanine exchange factor PDZ-GEF2, via its cytoplasmic type II PDZ-binding motif (Ebnet *et al.*, 2000; Severson *et al.*, 2009). Close apposition of the latter two signaling components in dimerized JAM-A appears to be necessary for activation of the small GTPase Rap1a, stabilization of β1 integrin, and regulation of cell migration (Severson *et al.*, 2009). Despite these findings linking JAM-A–mediated signaling to cell migration, the signaling events linking JAM-A to regulation of epithelial permeability are not known.

It is well appreciated that interactions of TJ-associated transmembrane proteins with large scaffold proteins and the actin cytoskeleton mediate regulation of paracellular permeability in a highly dynamic manner. Paracellular permeability to small molecules is directly determined by tetraspan claudins, which cluster as homodimers across cells to form channels of varying permeability to specific ions (Furuse, 1998; Nitta *et al.*, 2003; Furuse, 2010). Intriguingly, JAM-A-deficient cell lines and mice, which have enhanced intestinal permeability, also have altered expression of claudins 10 and 15, which regulate permeability to small solutes (Colegio *et al.*, 2003; Van Itallie *et al.*, 2003, 2006; Laukoetter *et al.*, 2007). The mechanisms defining how JAM-A regulates claudin 10/15 are not known, however, nor is it understood whether this observed alteration in claudin composition is sufficient to account for the enhanced permeability observed in JAM-A–deficient animals. On the other hand, paracellular permeability to larger molecules is regulated by the TJ-associated apical cytoskeleton, which responds to extracellular cues by expanding and contracting via actomyosin interactions (Madara and Pappenheimer, 1987; Nusrat *et al.*, 1995; Bruewer *et al.*, 2004). The contractile tone of the apical cytoskeleton is critical for maintaining a functional, polarized epithelium, and further stimulation of contraction has been shown to enhance paracellular flux of larger molecules by expanding the paracellular space (Shen *et al.*, 2006; Ivanov *et al.*, 2007). Despite an abundance of evidence showing intimate interactions between TJ proteins and the apical cytoskeleton (Madara and Pappenheimer, 1987; Nusrat *et al.*, 1995; Fanning *et al.*, 1998; Itoh *et al.*, 1999), the relationship between JAM-A and the apical cytoskeleton is not understood.

It is well appreciated that transmembrane TJ proteins communicate with the apical cytoskeleton through interactions with cytoplasmic scaffold or plaque proteins. Of interest, JAM-A has been reported to associate with actin-binding scaffold proteins ZO-1 and afadin (Bazzoni *et al.*, 2000; Ebnet *et al.*, 2000; Severson *et al.*, 2009), both of which are implicated in the regulation of barrier. ZO-1 and its closely related family member, ZO-2, regulate TJ assembly and play important roles in controlling epithelial permeability (Van Itallie *et al.*, 2009). Similarly, mice with intestinal epithelial–targeted loss of afadin demonstrate enhanced intestinal permeability (Tanaka-Okamoto *et al.*, 2011) with a phenotype similar to that observed in JAM-A–deficient mice, strengthening the notion of a functional link between JAM-A and afadin. Of importance, mice deficient in nectin, another afadin-associated adherens protein, did not demonstrate altered intestinal permeability (Tanaka-Okamoto *et al.*, 2011), suggesting that afadin may regulate barrier function downstream of JAM-A in a nectin-independent manner. Scaffold proteins such as afadin and the ZO proteins have several functional binding regions, such as PDZ domains, which associate with transmembrane proteins, actin-binding domains, and RA domains and can serve as binding sites for small GTPases (Mandai *et al.*, 1997; Yamazaki *et al.*, 2008; Van Itallie *et al.*, 2009). Given the foregoing observations, it is reasonable to assume that PDZ-dependent interactions between JAM-A and certain scaffold proteins may play important role(s) in regulating epithelial barrier function. The nature of such interactions, however, and the identity of signaling elements linking JAM-A to regulation of epithelial permeability remain unclear.

In this study, we use in vitro and in vivo techniques to better define mechanisms that link JAM-A to the regulation of epithelial barrier function. Our results suggest that JAM-A forms a complex with PDZ-containing scaffold proteins that regulates contractility of the apical cytoskeleton, which, in turn, fine tunes epithelial permeability. Of note, we report that the tight junction scaffold protein ZO-2 directly interacts with JAM-A and is necessary for mediating indirect interactions between JAM-A and afadin. We also show that JAM-A and afadin mediate activation of Rap2c, a GTPase previously uncharacterized in the context of epithelial barrier function. Taken together, these findings provide new insights into the regulation of epithelial barrier function by JAM-A.

RESULTS

JAM-A–binding reovirus protein σ1 induces JAM-A internalization and enhances permeability in vivo and in vitro

JAM-A–deficient mice and JAM-A–deficient intestinal epithelial cells display reduced TER and increased flux to 3- to 4-kDa dextrans (Laukoetter *et al.*, 2007), although mechanisms defining JAM-A regulation of epithelial permeability are not understood. To better understand the link between JAM-A and barrier function, we performed experiments comparing the role of JAM-A during TJ assembly/barrier formation with maintenance of a stable barrier. For these studies, we used a recombinant form of reovirus protein σ1, which has been shown to bind to the membrane-distal D1 domain of JAM-A and disrupt JAM-A homodimerization (Guglielmi *et al.*, 2007; Kirchner *et al.*, 2008; Zhang *et al.*, 2010). Addition of WT σ1 to subconfluent monolayers of model intestinal epithelial cell lines inhibited barrier development in comparison to cells treated with σ1_G381A mutant protein, which is deficient in JAM-A binding (Kirchner *et al.*, 2008; Figure 1A). In addition, incubation of confluent monolayers of SKCO-15 (Figure 1B) or T84 cells (Supplemental Figure S1A) with σ1 (20 μg/ml, 1 h for SK-CO15 cells and up to 3 h for T84 cells) resulted in a significant reduction in TER in comparison to confluent cells treated with σ1_G381A, suggesting that JAM-A regulates both assembly and maintenance of the epithelial barrier. Immunofluorescence labeling and confocal microscopy revealed that cells exposed to σ1 had reduced levels of TJ-associated JAM-A compared to cells incubated with σ1_G381A (Figure 1C); however, localization of E-cadherin was unaffected (Supplemental Figure S1B), suggesting that effects observed were specific to JAM-A and epithelial architecture remained intact. To assess the in vivo significance of the in vitro findings, we examined the effect of σ1 on intestinal permeability in anesthetized mice. With an intestinal loop model, administration of σ1 into the intestinal lumen for 2 h resulted in a fourfold increase in permeability to 3-kDa dextran compared to treatment with σ1_G381A (Figure 1D). These findings suggest that reduction of TJ-associated JAM-A after σ1 exposure compromises TJ barrier function.

Because exposure of intestinal epithelial cells to σ1 resulted in a reduction of TJ-associated JAM-A and concomitant barrier defects similar to that observed in knock-out mice, we initiated experiments to better define JAM-A–dependent mechanisms regulating barrier function using epithelial cell lines deficient in JAM-A. As can be seen in Supplemental Figure S1C, stable intestinal epithelial cells (IECs) deficient in JAM-A displayed delayed development of TER compared to control nonsilenced (NS) IECs.

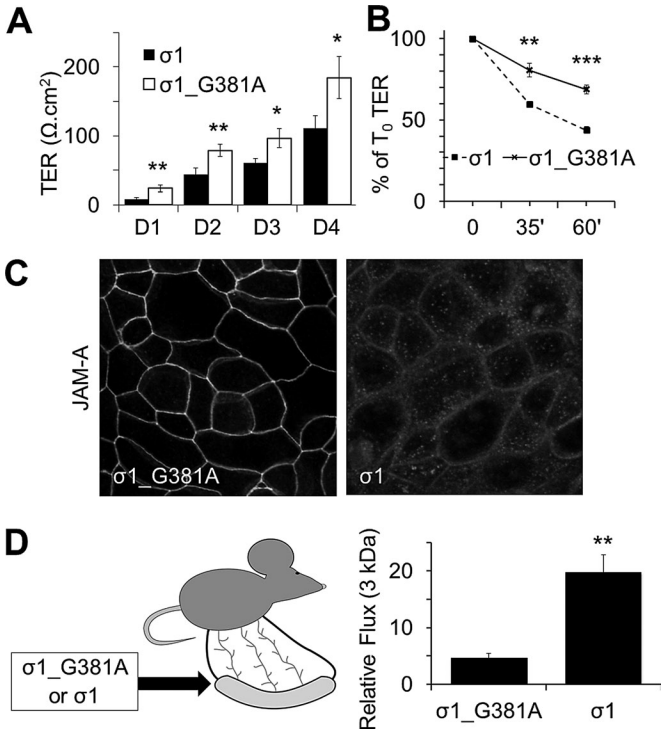

FIGURE 1: JAM-A regulates barrier function. (A) Treatment of SK-CO15 with σ1 (10 μg/ml) on plating abrogates the formation of TER compared to cells treated with mutant σ1_G381A (representative experiment with three independent samples; mean ± SD). (B) Treatment of confluent SK-CO15 monolayers with σ1 (20 μg/ml) for 1 h led to significant reduction in TER compared to cells treated with σ1_G381A mutant (representative experiment with three independent samples; mean ± SD). (C) Treatment of confluent SK-CO15 monolayers with σ1 (20 μg/ml) for 1 h led to significant reduction in JAM-A expression at tight junctions. (D) Administration of σ1 in vivo enhances permeability to small molecules. WT σ1 or σ1_G381A (100 μg/ml) was administered to intestinal loops of WT mice for 1 h and then assessed for 3-kDa dextran flux for another hour ($n = 3$ per group; mean ± SEM). For all experiments, $*p < 0.05$, $**p < 0.01$, $***p < 0.001$ between groups at each time point per Student's *t* test.

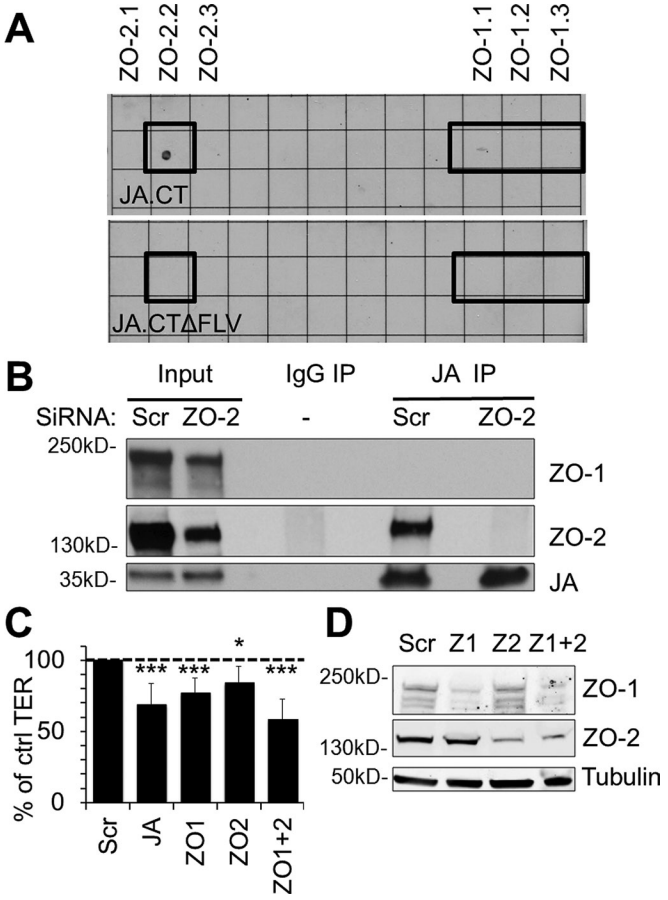

FIGURE 2: JAM-A associates with ZO-2, an important component of barrier function. (A) JAM-A interacts with ZO-2 in vitro. A proteomic array containing 96 PDZ domains from 48 different proteins was used to screen for proteins interacting with the cytoplasmic PDZ-binding motif of JAM-A. The recombinant full-length cytoplasmic tail of JA (JA.CT) directly interacted with the second PDZ domain of ZO-2 on the array but did not detectably interact with any PDZ domains of ZO-1. In contrast, a mutant lacking the PDZ-binding motif on the cytoplasmic tail of JAM-A (JA.CTΔFLV) failed to interact with ZO-2. (B) JAM-A (JA) coimmunoprecipitates with ZO-2 but not ZO-1 in intestinal epithelial cells. JAM-A immunoprecipitates from cell lysates prepared with an NP40-based buffer revealed a 160-kDa ZO-2 immunoreactive band. siRNA down-regulation of ZO-2 was used to confirm specificity of the detected band. (C) Down-regulation of ZO-1, ZO-2, or ZO-1 and -2 led to decreased TER in SK-CO15 cells at similar levels to down-regulation of JAM-A relative to control cells (Scr; $n > 5$; mean relative resistance with 95% confidence interval). (D) siRNA-mediated down-regulation of ZO-1 and/or ZO-2 was confirmed by immunoblotting.

JAM-A interacts directly with the TJ plaque protein ZO-2

Because loss of JAM-A at the apical junctional complex disrupted barrier development and maintenance, we sought to identify JAM-A–associated effector proteins that regulate epithelial permeability. JAM-A interacts with several scaffold proteins through its C-terminal PDZ binding motif (Nomme *et al.*, 2011). We screened for PDZ-dependent binding of the recombinant full-length cytoplasmic segment of JAM-A (amino acids 261–300) using a proteomic array of 96 recombinant PDZ domains derived from 48 distinct scaffold proteins. Analyses of array results revealed binding of glutathione *S*-transferase (GST)–tagged cytoplasmic tail of JAM-A to the second PDZ domain of ZO-2. Specificity for a PDZ-dependent interaction was confirmed by absence of ZO-2 binding to a GST-tagged JAM-A cytoplasmic tail mutant protein lacking the distal PDZ-binding motif (Figure 2A). Of interest, we observed in vitro interactions of the full-length JAM-A cytoplasmic domain with the second PDZ domain of ZO-2 but not with any of the three PDZ domains of ZO-1 despite previous reports suggesting a direct interaction between JAM-A and the third PDZ domain of ZO-1 (Nomme *et al.*, 2011). To test whether full-length JAM-A and ZO-2 interact in epithelial cells, we performed coimmunoprecipitation assays for ZO-2 and JAM-A from lysates of polarized human IECs. Western blots of JAM-A immunoprecipitates prepared with buffers containing various detergents including NP40 alone or a mixture of Triton X-100, sodium deoxycholate, and SDS (RIPA) revealed a prominent 160-kDa band immunoreactive with ZO-2 antibodies (Figure 2B and Supplemental Figure S2, respectively). Small interfering RNA (siRNA)–mediated knockdown of ZO-2 resulted in loss of the 160-kDa protein band, confirming the identity of the coimmunoprecipitating protein as ZO-2 (Figure 2B). We were unable, however, to detect JAM-A association with ZO-1 using the same coimmunoprecipitation procedure in SK-CO15 and T84 cells (Figure 2B and Supplemental Figure S2), despite robust coimmunoprecipitation of ZO-1 with

ZO-2 in the same experiment (Supplemental Figure S2). Finally, we investigated the localization of ZO-2 in epithelial cells treated with σ1, which decreased levels of junction-associated JAM-A in Figure 1C. As shown in Supplemental Figure S2B, σ1 treatment also perturbed junctional localization of ZO-2, as assessed by confocal immunofluorescence imaging.

Given the array findings in Figure 2A and results in Figure 2B and Supplemental Figure S2B demonstrating association of JAM-A with ZO-2, we assessed whether down-regulation of JAM-A and ZO-1/2 might have similar negative effects on barrier function. Transient down-regulation of ZO-1 and ZO-2 in isolation or together resulted in decreased TER to levels similar to those observed after transient down-regulation of JAM-A (Figure 2, C and D). The similar effects on TER observed after down-regulation of JAM-A and ZO proteins, along with results demonstrating JAM-A association with ZO-2, suggest that JAM-A and ZO proteins may be part of a common signaling pathway to regulate barrier function.

Afadin and PDZ-GEF1, but not PDZ-GEF2 or Rap1, regulate epithelial barrier function

To identify other JAM-A effectors that regulate barrier function, we evaluated several signaling proteins that have been shown to play roles in JAM-A–mediated control of cell migration. Specifically, we tested whether afadin, PDZ-GEF2, and Rap1a, components of the pathway linking JAM-A to regulation of epithelial cell migration, could also affect barrier function (Severson *et al.*, 2009). Transient, siRNA-mediated down-regulation of afadin caused a significant decrease in TER compared to cells transfected with scrambled siRNA. In contrast, siRNA-mediated down-regulation of PDZ-GEF2 did not impair epithelial permeability (Figure 3A). However, down-regulation of PDZ-GEF1, a closely related homologue of PDZ-GEF2, resulted in significantly decreased TER comparable to that observed after down-regulation of JAM-A (Figure 3A). We then performed experiments to examine the barrier-modulating roles of Rap1a or Rap1b, small GTPases that are known downstream target proteins of PDZ-GEF1/2 (Pannekoek *et al.*, 2011). Surprisingly, we observed that transient down-regulation of Rap1a and Rap1b did not decrease TER in IECs (Figure 3A). Given the similar TER effects observed after down-regulation of JAM-A and PDZ-GEF1, we performed coimmunoprecipitation experiments to see whether the two proteins are components of the same protein complex. PDZ-GEF1 immunoprecipitates from IEC lysates revealed a 37-kDa protein band that was immunoreactive with JAM-A antibody (Figure 3B), indicating that JAM-A is in a complex with PDZ-GEF1. Furthermore, using confocal microscopy and immunofluorescence staining, we observed that PDZ-GEF1 localized to epithelial junctions (Figure 3C), as previously reported for afadin, another scaffold protein shown to be in a complex with JAM-A (Ebnet *et al.*, 2000; Severson *et al.*, 2009; Tanaka-Okamoto *et al.*, 2011). These results suggest that afadin and PDZ-GEF1 associate with JAM-A in the apical junctional complex.

We previously reported association between JAM-A and afadin (Severson *et al.*, 2009) and confirmed that JAM-A is present in afadin immunoprecipitates of polarized IECs (Figure 3B). Of importance, we observed that afadin immunoprecipitates revealed two protein bands of close molecular weight that were immunoreactive with JAM-A antibodies. It is likely that the JAM-A doublet observed in afadin immunoprecipitates represents two differentially phosphorylated forms of JAM-A, as described in the literature (Iden *et al.*, 2012). On the basis of this previous report, it is possible that the higher–molecular weight species, which is of the same size as the single JAM-A band observed in immunoprecipitates of PDZ-GEF1 (Figure 3B), represents phosphorylated, tight-junction–associated JAM-A.

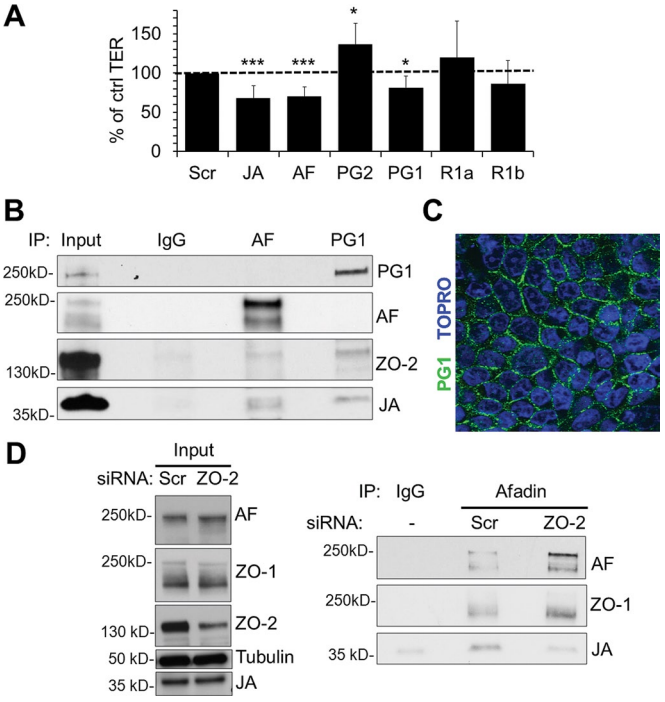

FIGURE 3: Down-regulation of afadin and PDZ-GEF1, but not PDZ-GEF2 or Rap1a/b, leads to decreased resistance across IECs. (A) Transient down-regulation of afadin (AF) and PDZ-GEF1 (PG1) reduced intestinal epithelial TER to levels comparable to those observed after transient JAM-A down-regulation (JA). Down-regulation of PDZ-GEF2 (PG2), Rap1a (R1a), and Rap1b (R1b) did not affect intestinal epithelial TER ($n > 4$; mean relative resistance with 95% confidence interval; data for JAM-A from Figure 2). (B) JAM-A (JA) and ZO-2 coimmunoprecipitate with PDZ-GEF1 (PG1) and afadin (AF) in IECs. Cell lysates were preextracted with an NP40-based buffer, and pellets were resuspended in RIPA buffer before coimmunoprecipitation with PDZ-GEF1 or afadin. (C) PDZ-GEF1 localizes to the perijunctional region of IECs. (D) JAM-A (JA) coimmunoprecipitation with afadin (AF) is disrupted after transient down-regulation of ZO-2. Cell lysates were prepared with a Brij97-based buffer before coimmunoprecipitation with afadin.

Of interest, the same afadin immunoprecipitates also revealed a 160-kDa band immunoreactive for ZO-2. Because our results suggest that afadin and PDZ-GEF1 are in a complex with ZO-2 and JAM-A, we performed experiments to gain further insight into which of these proteins might directly or indirectly interact with JAM-A. The in vitro PDZ array results in Figure 2A suggest that JAM-A might directly interact with ZO-2. We thus performed experiments to determine whether the association between JAM-A and afadin depended on ZO-2. Analyses of afadin immunoprecipitates from cells treated with either scrambled or ZO-2 siRNA revealed coimmunoprecipitation of JAM-A with afadin in control cells, but the protein association was greatly diminished in IECs after transient siRNA-mediated depletion of ZO-2 (Figure 3D). In contrast, loss of ZO-2 had no effect on the coimmunoprecipitation of ZO-1 with afadin. Combined with the findings in Figure 2, these results suggest that afadin association with JAM-A depends on ZO-2, whereas afadin association with ZO-1 is independent of ZO-2. These findings support a model in which JAM-A binds directly with ZO-2 and indirectly associates with afadin and ZO-1.

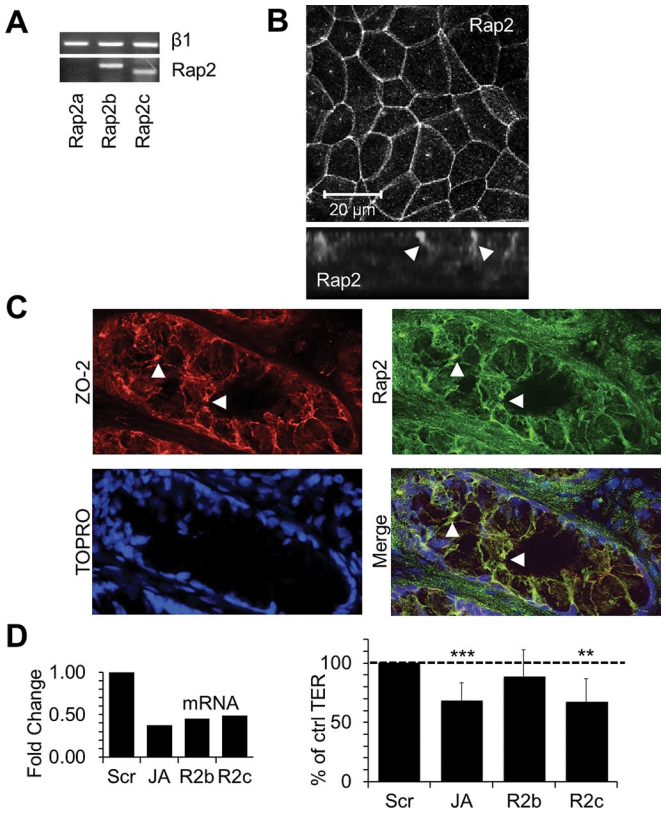

FIGURE 4: Rap2 is expressed in the apical spaces between IECs, and Rap2c is involved in the regulation of intestinal epithelial barrier function. (A) mRNAs for Rap2 subtypes Rap2b and Rap2c but not Rap2a are present in SK-CO15 cells, as observed by PCR. RNA was extracted from confluent SK-CO15 cells and subjected to RT-PCR. A common cDNA template and PCR master mix was prepared and then subdivided before addition of Rap2a, Rap2b or Rap2c primers. (B) Rap2 protein is present in apical intercellular junctions of SK-CO15 cells. (C) Rap2 colocalizes with the tight junction marker ZO-2 in colonic mucosa from human pathology specimens. Tissue sections were pretreated with 0.1% Triton X-100 before fixation. (D) qRT-PCR–verified down-regulation of Rap2c (R2c) but not Rap2b (R2b) led to significant reductions in colonic epithelial TER at levels comparable to those observed after transient JAM-A down-regulation (JA; $n > 5$; relative mean resistance with 95% confidence interval; data for JAM-A from Figure 2).

Rap2c localizes to apical cell contacts and regulates epithelial paracellular permeability downstream of JAM-A

Given the observed association between JAM-A and PDZ-GEF1 and the similar effects on permeability observed after siRNA-mediated down-regulation of these two proteins, we performed experiments to identify putative barrier-regulating GTPases that might be activated by PDZ-GEF1 downstream of JAM-A. As shown in Figure 3A, down-regulation of Rap1a or Rap1b did not decrease TER in IECs, and thus we evaluated other PDZ-GEF substrates. Specifically, we assessed a role for Rap2, the only other known substrate for PDZ-GEF1 (De Rooij *et al.*, 1999). PCR analyses revealed that SK-CO15 cells expressed mRNA for Rap2 subtypes Rap2b and Rap2c but not Rap2a, as confirmed by two sets of Rap2a primers (Figure 4A and Supplemental Figure S4). To confirm protein expression, we performed immunofluorescence staining and confocal microscopy on SK-CO15 cells and demonstrated that Rap2 localized to apical cell–cell contacts (Figure 4B). Additional immunofluorescence staining and confocal microscopy of native human colonic epithelium revealed that Rap2 localized along cell borders and colocalized with ZO-2 at apical cell junctions, consistent with TJ localization. On the basis of these results, we performed experiments to evaluate the role of Rap2b and Rap2c in regulating epithelial barrier function. Transient down-regulation of Rap2c, but not Rap2b, using two separate siRNA targets for each gene resulted in decreased TER similar to that observed after transient JAM-A down-regulation (Figure 4D). Further analyses of Rap2 expression revealed colocalization of Rap2 with JAM-A in cultured epithelial cells in vitro (Figure 5A) and native human colonic epithelium (Figure 5B). Given that JAM-A and Rap2 colocalized at junctions and had similar effects on TER, we hypothesized that Rap2c and JAM-A may share a common signaling pathway. To better define the role of Rap2c as a putative JAM-A effector protein that regulates barrier function, we performed double JAM-A, Rap2c–knockdown studies. Simultaneous down-regulation of Rap2c and JAM-A had no further additive effect on TER compared to down-regulation of Rap2c or JAM-A in isolation (Figure 5C). Given the observations suggesting that afadin and JAM-A are components of a protein complex that regulates TER and that afadin contains a GTPase-binding site, we examined whether JAM-A and afadin also shared a common role in regulating the small GTPase Rap2. We thus assessed Rap2 activity using RalGDS binding assays in stable cell lines deficient in JAM-A and in cells transiently depleted of afadin. As shown in Figure 5, D and E, Rap2 activity was reduced in JAM-A–deficient (Figure 5D) and afadin-deficient (Figure 5E) cells. We next assessed whether Rap2 was part of a protein complex containing JAM-A and afadin. Because afadin contains a GTPase-binding site, we probed immunoprecipitates of afadin from lysates of polarized IECs for Rap2, as shown in Figure 5F. Together with our findings demonstrating JAM-A colocalization with Rap2 (Figure 5A), these results suggest that Rap2 is in a protein complex with JAM-A and afadin. Finally, given our findings implicating regulation of Rap2 activity by JAM-A and afadin, as well as the observed coimmunoprecipitation of Rap2 with afadin, we performed experiments to determine whether the subcellular localization of Rap2c is also regulated by JAM-A. Confluent IECs transiently expressing FLAG-tagged Rap2c were incubated with reovirus protein σ1 to induce JAM-A localization away from TJs, as highlighted in Figure 1C. Compared to incubation with JAM-A binding deficient mutant σ1_G381A, IECs exposed to σ1 for 1 h demonstrated a loss of junction-associated Rap2c (Figure 5G). These findings suggest that JAM-A plays a role in mediating Rap2c distribution in cell junctions and that this complex is important for Rap2 activation.

Loss of JAM-A increases epithelial paracellular permeability to high–molecular weight molecules

Because afadin, ZO-1, and ZO-2 have known actin-binding sites (Mandai *et al.*, 1997) and Rap2 activity has been implicated in cytoskeletal regulation in neurons and enterocytes (Ryu *et al.*, 2008; Gloerich *et al.*, 2012), we considered whether JAM-A–dependent regulation of barrier function may involve Rap2c-mediated effects on the actin cytoskeleton. We first examined whether loss of JAM-A in vivo and in vitro resulted in barrier defects consistent with cytoskeletal deregulation. Whereas permeability to small molecules is largely dependent on the composition and stability of claudin-forming pores (Nitta *et al.*, 2003), paracellular passage of larger molecules is determined by expansion of the paracellular space secondary to regulation of the apical cytoskeleton (Nusrat *et al.*, 1995, 2000; Jou *et al.*, 1998; Shen *et al.*, 2011). Previous studies showed that JAM-A-knockout (KO) mice have increased intestinal epithelial permeability to small molecules (4-kDa dextran; Laukoetter *et al.*,

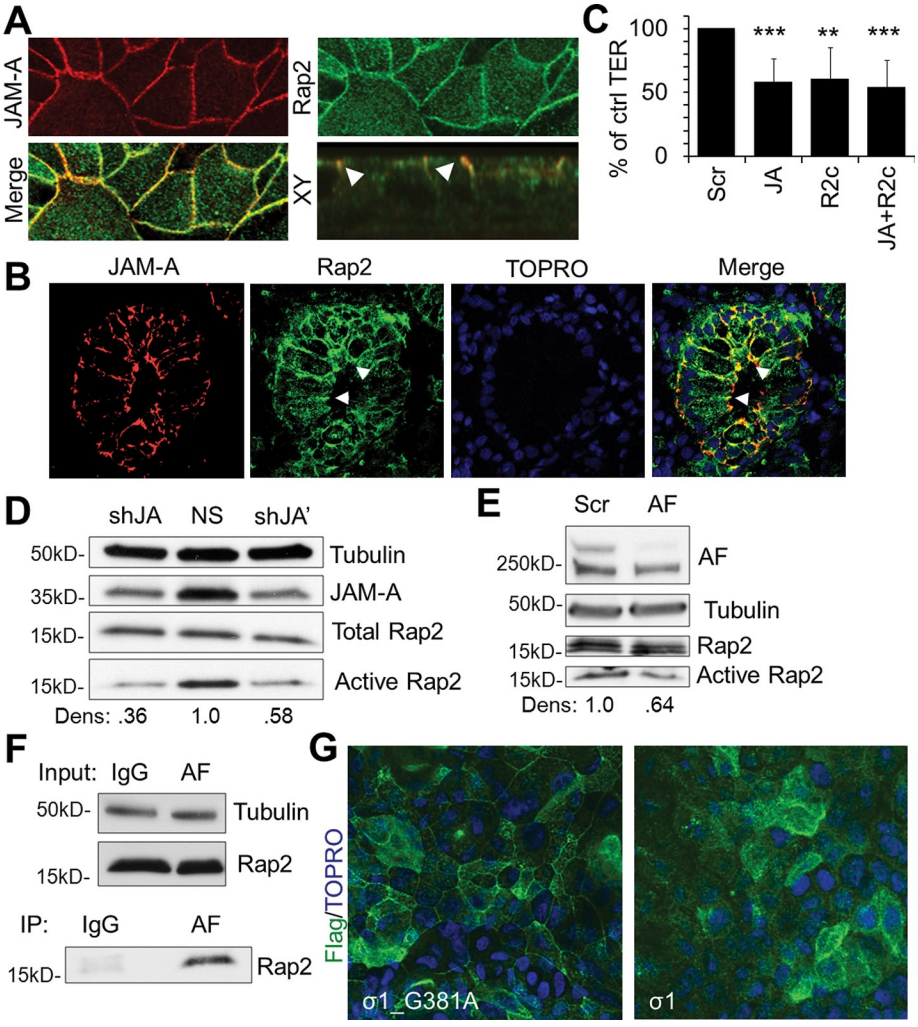

FIGURE 5: JAM-A regulates Rap2 activity and localization to tight junctions. (A) Rap2 colocalizes with JAM-A (JA) in IECs and (B) in colonic mucosa from human pathology specimens. (A, B) Cells and tissues were pretreated with 0.1% Triton X-100 before fixation. (C) Simultaneous down-regulation of JAM-A (JA) and Rap2c (R2c) in SK-CO15 cells has no additive effect on TER compared to isolated down-regulation of JAM-A (JA) or Rap2c (R2c; $n = 3$; mean relative resistance with 95% confidence interval). (D) JAM-A (JA)–deficient IECs from two independent JAM-A targets display decreased Rap2 activity compared to control cells (NS), as assessed by Ral-GDS pull down (densitometry calculated as Rap2 pull-down signal over total Rap2 signal, relative to NS control). (E) IECs transiently deficient in afadin (AF) have decreased levels of Rap2 activity compared to control cells (Scr; densitometry calculated as Rap2 pull-down signal over total Rap2 signal, relative to Scr control). (F) Rap2 coimmunoprecipitates with afadin from cell lysates solubilized with a Brij97-based buffer. (G) Incubation of confluent SK-CO15 monolayers with σ1 or σ1_G381A (10 μg/ml) for 1 h leads to decreased Rap2c localization at tight junctions.

2007). However, intestinal permeability to larger solutes, which would indicate a role for cytoskeletal regulation of barrier function, has not been assessed in these animals. We thus investigated the role of JAM-A in the regulation of permeability to large molecules in an intestinal loop model using anesthetized mice (setup illustrated in Figure 1D). Introduction of 40-kDa dextran to the intestinal lumen of JAM-A KO mice demonstrated a sixfold increase in intestinal permeability compared to values obtained in wild-type (WT) animals (Figure 6A), suggesting a potential role for cytoskeletal regulation of JAM-A–dependent barrier function. We also tested whether cell lines with stable JAM-A knockdown had increased permeability to high–molecular weight dextran (40 kDa). As shown in Figure 6B, in vitro flux of 40-kDa dextran across monolayers of JAM-A deficient cells was significantly increased compared to nonsilenced cells. Given the observed association between ZO-2 and JAM-A and that loss of either protein elicited similar effects on TER, we also assessed the effect of ZO-2 down-regulation on permeability to high–molecular weight molecules. As shown in Figure 6C, transient down-regulation of ZO-2 in IECs led to a significant increase in 40-kDa dextran flux relative to scramble siRNA–transfected cells, confirming previous observations that ZO-2 also plays a role in regulating permeability to high–molecular weight molecules in epithelial cells (Hernandez *et al.*, 2007).

JAM-A down-regulation leads to RhoA-mediated cell contraction

Given the enhanced permeability to large molecules observed with in vivo and in vitro JAM-A deficiency, we investigated whether JAM-A played a role in the regulation of perijunctional actin turnover or apical actomyosin contraction. To test whether JAM-A expression plays a role in actin turnover, we examined fluorescence recovery after photobleaching (FRAP) in IECs transfected with actin–green fluorescent protein (GFP). In these experiments, segments of perijunctional actin-GFP were photobleached by at least 50% in control and JAM-A–deficient IECs followed by analysis of the rate of fluorescence recovery. As shown in Figure 6D, FRAP experiments revealed similar rates of recovery between control and JAM-A–deficient cells, suggesting that JAM-A does not regulate epithelial permeability by affecting actin turnover. We next asked whether JAM-A loss results in altered actomyosin contractility. Given our findings linking JAM-A–dependent barrier function to afadin (Figure 3) and previous reports linking afadin to regulation of RhoA (Miyata *et al.*, 2009), a small GTPase reported to enhance apical cytoskeleton contraction and increase permeability in IECs and endothelial cells (Nusrat *et al.*, 1995; Hirase *et al.*, 2001), we examined whether JAM-A–deficient cells had altered RhoA activity. As shown in Figure 6E, JAM-A–deficient cell lines exhibited increased RhoA activity compared to NS controls. Because RhoA is implicated in regulation of actomyosin contraction through phosphorylation of nonmuscle myosin 2 (pMLC), we examined levels of pMLC in JAM-A–deficient IECs by Western blot. Compared to NS controls, JAM-A–deficient stable cell lines exhibited higher levels of pMLC (Figure 6F). To confirm that changes in pMLC observed in cell lysates reflected signaling at the level of the cortical actomyosin belt, we assessed localization of pMLC in JAM-A–deficient stable cell lines by immunofluorescence staining. As shown in Figure 6G, JAM-A–deficient IECs exhibited enhanced perijunctional pMLC staining compared to NS cells. These observations suggest that JAM-A may regulate barrier function through RhoA-mediated effects on the

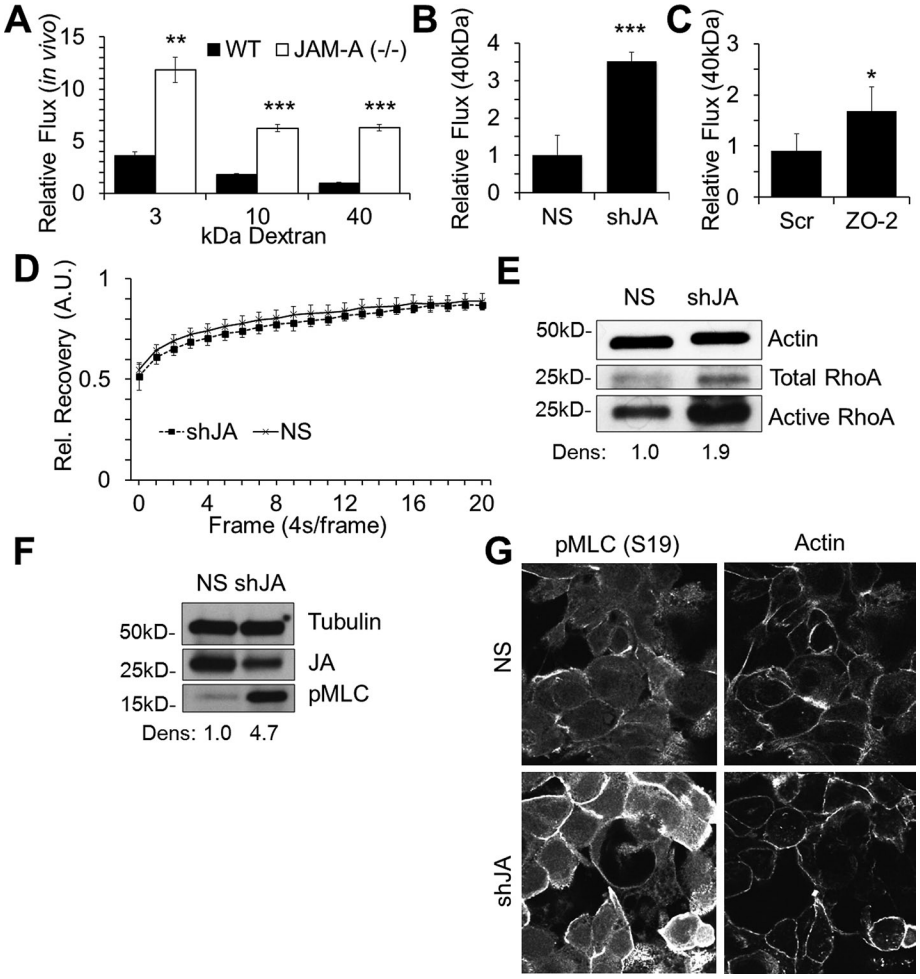

FIGURE 6: JAM-A down-regulation enhances cytoskeletal contraction. (A) JAM-A$^{-/-}$ mice exhibit increased intestinal permeability to 3-, 10-, and 40 kDa dextran compared to WT mice ($n = 3$; bars, mean ± SEM). (B) JAM-A–deficient SK-CO15 cells (shJA) demonstrate enhanced flux to 40-kDa dextran compared with control cells (NS). Dextran flux to the bottom chamber was assessed after 2 h (representative experiment with three independent sample; mean ± SD). (C) Transient down-regulation of ZO-2 in IECs results in enhanced permeability of 40-kDa dextran compared to control (Scr; representative experiment with three independent samples; mean ± SD). (D) Actin turnover rates in control (NS) or JAM-A deficient (shJA) cells are not statistically different, as assessed by FRAP. Stable control (NS) or JAM-A deficient (shJA) cells expressing actin-GFP and grown in chambered wells before assessment of FRAP for actin-GFP at junctions (n = 8; mean ± SEM). (E) Stable down-regulation of JAM-A (shJA) leads to enhanced levels of total and active RhoA as determined by Rhotekin pull-down assay (densitometry calculated as RhoA pull-down signal over total RhoA signal, relative to NS control). (F, G) Stable down-regulation of JAM-A (shJA) leads to enhanced levels of pMLC (S19) as determined by Western blot (F; densitometry calculated as pMLC signal over tubulin signal, relative to NS control) and confocal immunofluorescence staining (G).

contractility of the actomyosin belt without influencing mobility of perijunctional actin. From these findings we propose a model highlighting a signaling module downstream of JAM-A that regulates epithelial barrier function (Figure 7).

DISCUSSION

In this study, we provide new mechanistic insights into how JAM-A regulates epithelial barrier function. Whereas previous reports implicated JAM-A in the control of barrier (Liang *et al.*, 2000; Laukoetter *et al.*, 2007), the signaling pathways linking JAM-A to regulation of epithelial permeability were not defined. We used a variety of in vitro and in vivo approaches to find that JAM-A is part of a complex containing ZO-2, afadin, and PDZ-GEF1 that regulates activation of Rap2c and actomyosin contraction via RhoA.

To identify JAM-A–associated scaffold proteins that may play a role in regulating epithelial permeability, we screened a library of PDZ domain–containing scaffold proteins for interaction with recombinant cytoplasmic JAM-A. We observed direct binding of the cytoplasmic region of JAM-A to the second PDZ domain of ZO-2 and confirmed this interaction by demonstrating coimmunoprecipitation of ZO-2 with JAM-A from cell lysates derived from polarized human IECs. This is the first report of an association between JAM-A and ZO-2. Of interest, our results did not demonstrate interaction between JAM-A and ZO-1, in contrast to earlier reports (Ebnet *et al.*, 2000; Nomme *et al.*, 2011). As can be seen in Figure 2 and Supplemental Figure S2, there was robust coimmunoprecipitation of ZO-2 with JAM-A using lysates from two polarized, nontransfected, human IECs (SK-CO15 and T84) under different detergent conditions. Although these findings suggest a direct interaction between JAM-A and ZO-2, given the conserved nature of PDZ-dependent interactions, it is not surprising that ZO-1 has been reported to associate with JAM-A. For example, a recent crystallography study reporting a direct interaction between JAM-A and ZO-1 was based on experiments using micromolar concentrations of cytoplasmic segments of JAM-A and the third PDZ domain of ZO-1 (Nomme *et al.*, 2011). In comparison, our observations were based on in vitro interactions between nanomolar concentrations of cytoplasmic JAM-A segments and the second PDZ-domain of ZO-2. Because sequence alignment between the third PDZ domain of ZO-1 and the second PDZ domain of ZO-2 shows >40% identity (Altschul *et al.*, 1997, 2005), it is not unreasonable to expect that a cytoplasmic segment of JAM-A that directly binds to ZO-2 could also associate with ZO-1 at higher concentrations. The most plausible explanation for our results using polarized IECs, however, is that JAM-A directly interacts with ZO-2, whereas indirect interactions between JAM-A and ZO-1 may be mediated through known associations between ZO-1 and ZO-2 (Gumbiner *et al.*, 1991).

We performed further experiments to define JAM-A effectors involved in regulating barrier from insights obtained from previous studies on JAM-A regulation of cell migration. We observed that transient down-regulation of afadin but not PDZ-GEF2 or Rap1a/b reduced TER. Although we were not able to show a role for PDZ-GEF2 in barrier maintenance, we observed that loss of the closely related PDZ-GEF1 resulted in enhanced permeability similar to what was observed with JAM-A loss. Because the association with PDZ-GEF1 had not been previously defined, we performed coimmunoprecipitations

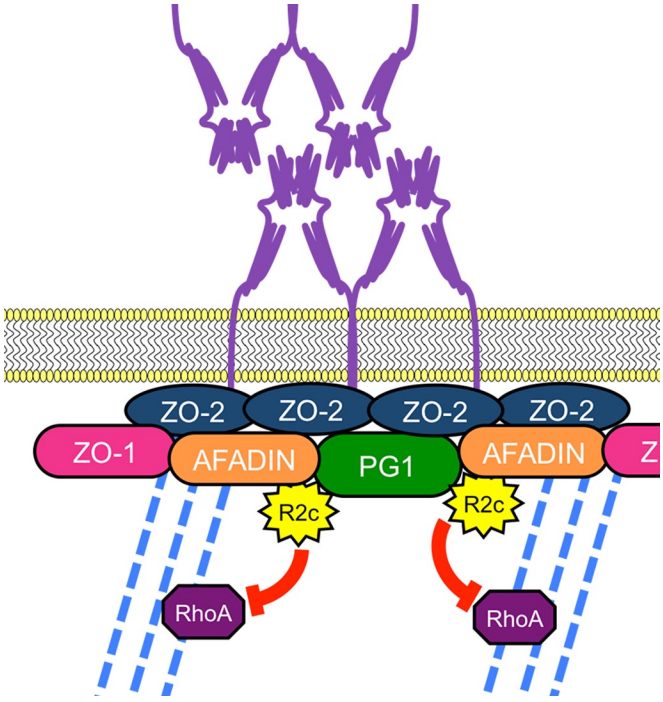

FIGURE 7: Model of JAM-A–mediated barrier function. We propose that JAM-A is part of a complex composed of ZO-2, afadin, and PDZ-GEF1 (PG1) that recruits and activates Rap2c (R2c) and controls actomyosin contraction via RhoA activation to regulate epithelial barrier function.

that demonstrated interaction between JAM-A and PDZ-GEF1. It is noteworthy that a direct interaction between JAM-A and PDZ-GEF1 was not observed in the proteomic PDZ array, even though the PDZ domain of PDZ-GEF1 was probed, suggesting that the association between PDZ-GEF1 and JAM-A is likely indirect and/or transient in nature.

Immunoprecipitation of afadin not only confirmed association between afadin and JAM-A, but it also revealed an association between afadin and ZO-2. Given the observed interactions between JAM-A and PDZ-GEF1, afadin, and ZO-2 and previously reported interactions of ZO-1 with ZO-2 (Gumbiner *et al.*, 1991) and afadin (Takahashi *et al.*, 1998), we sought to further define the order of association between proteins in this complex. On the basis of findings from the PDZ array and coimmunoprecipitations indicating a potential direct interaction between JAM-A and ZO-2, we tested whether the association of afadin with JAM-A depended on ZO-2 expression. Transient down-regulation of ZO-2 followed by afadin immunoprecipitation revealed that IECs deficient in ZO-2 demonstrated decreased association between JAM-A and afadin. This suggested that JAM-A, ZO-2, and afadin were in a complex and the interaction between afadin and JAM-A required the presence of ZO-2. These results, which support an indirect association between afadin and JAM-A, are inconsistent with a previous study supporting a direct interaction between afadin and JAM-A (Ebnet *et al.*, 2000). We attribute these divergent interpretations to differences in experimental models. The earlier study was largely based on overexpression of proteins in yeast that were confirmed using recombinant protein–based pull-down assays, whereas the results of our proteomic screen were supported through antibody-based analyses of lysates from polarized human IECs containing endogenous levels of JAM-A, ZO-2, and afadin. The former study also demonstrated coimmunoprecipitation of afadin with JAM-A in endothelial cell lysates (Ebnet *et al.*, 2000), which is consistent with our previous observations in lysates of IECs (Severson *et al.*, 2009); however, these coimmunoprecipitation results do not distinguish between direct or indirect interactions. Considering the present finding that ZO-2 depletion in IECs attenuates association between JAM-A and afadin, our results suggest that JAM-A associates directly with ZO-2 and indirectly with afadin. The foregoing experiments also revealed that association between afadin and ZO-1 was not altered upon ZO-2 depletion, suggesting that ZO-2 is not required for the interaction between afadin and ZO-1. Given these observations and previous reports on ZO-1 interacting partners, we predict that ZO-1 may indirectly associate with JAM-A via interactions with afadin and/or ZO-2.

It was surprising to find that down-regulation of Rap1a/b did not enhance epithelial permeability. Rap1 is important in the regulation of endothelial tight junctions (Kooistra *et al.*, 2007; Pannekoek *et al.*, 2011). The role of Rap1 in epithelial barrier, however, has not been clearly defined (Monteiro and Parkos, 2012). Whereas others have shown a role for Rap1 effectors such as EPAC and RAPGAP in the regulation of the apical junctional complex in epithelial cells, such effectors have not been reported to be specific for Rap1 and, in fact, have been observed to modulate Rap2 signaling (De Rooij *et al.*, 1999; Roscioni *et al.*, 2008; Tsygankova *et al.*, 2010; Monteiro and Parkos, 2012). Here we report that Rap2c, a previously uncharacterized GTPase in epithelial cells, mediates JAM-A regulation of epithelial permeability.

Rap2a, but not Rap2c, was recently reported to play an important role in brush border formation in small intestinal enterocytes (Gloerich *et al.*, 2012). Moreover, Rap2 modulation was required for ordered formation of neuronal dendritic spines (Ryu *et al.*, 2008). Such reports suggest that Rap2 is important in regulating actin architecture, as observed for other members of the Ras superfamily of GTPases (McLeod *et al.*, 2004; Noda *et al.*, 2010). Of interest, mRNA for Rap2b and Rap2c but not for Rap2a was present in SKCO-15 cells, which helped to define a role for Rap2c in IECs. We observed that Rap2 colocalizes with JAM-A at the apical junctional complex and that Rap2 activity depends on JAM-A expression. In addition, PDZ-GEF1, shown in this report to associate with JAM-A, is an established activator of Rap2 (De Rooij *et al.*, 1999; Kuiperij *et al.*, 2003). We also performed experiments testing whether Rap2 activity was regulated by afadin, another JAM-A–associated plaque protein. We found that transient down-regulation of afadin led to decreased activity of Rap2 in IECs (Figure 5C), and, along with coimmunoprecipitation results in Figure 3B, these data collectively suggest that JAM-A forms a complex with ZO-2, afadin, and PDZ-GEF1 to regulate Rap2 activity, as highlighted in the model proposed in Figure 7.

We performed a series of experiments to determine how the proposed signaling complex in Figure 7 regulates epithelial permeability. We previously observed decreased TER and increased flux of 4-kDa dextran in JAM-A–null mice and demonstrated that JAM-A–null mice exhibited increased protein levels of claudins 10 and 15 (Laukoetter *et al.*, 2007). In this study, we report that JAM-A deficiency also results in an enhanced permeability to large molecules, suggesting that additional mechanisms, including altered regulation of the actin cytoskeleton, may be important in JAM-A–mediated regulation of barrier function. We observed that stable cell lines deficient in JAM-A had enhanced activity of RhoA and increased phosphorylation of myosin light chain. These observations complement previous reports indicating that afadin-deficient cells exhibited enhanced RhoA activity (Miyata *et al.*, 2009) and that epithelial cells deficient in ZO-1/2 revealed enhanced pMLC at the apical

junctional complex (AJC) compared to control cells, as assessed by immunofluorescence confocal microscopy of actin and myosin light chain (Fanning *et al.*, 2012).

The findings in this study have significant physiological relevance. Transient and incomplete down-regulation of JAM-A, ZO-1/2, afadin, PDZ-GEF1, and Rap2c in vitro led to TER decreases of ~15–45% compared to control groups. These relatively small in vitro differences observed in JAM-A deficient cells translated to threefold (small molecules) and sixfold (large molecules) increases in intestinal permeability in JAM-A KO relative to WT mice. Similarly, afadin cKO mice were reported to exhibit a threefold increase in permeability to low– molecular weight dextran, although permeability of high–molecular weight solutes was not reported. Although in vivo permeability data are not available for all protein targets that we studied in vitro, given that transient down-regulation of JAM-A, afadin, PDZ-GEF1, and rap2c led to statistically similar effects on TER in vitro, we predict that mice with epithelial-targeted deficiency of PDZ-GEF1 or rap2c may have barrier defects similar to those observed in JAM-A– and afadin-deficient mice. There are significant physiological consequences secondary to the permeability defects observed in JAM-A– and afadin-deficient mice. Mice lacking intestinal epithelial afadin (Tanaka-Okamoto *et al.*, 2011) or JAM-A (Laukoetter *et al.*, 2007) have higher susceptibility to dextran sodium sulfate–induced colitis. Moreover, we also showed that JAM-A–deficient mice develop immune-compensatory mechanisms to protect them against the development of spontaneous colitis secondary to enhanced antigen exposure (Khounlotham *et al.*, 2012). Such studies highlight the physiological ramifications of JAM-A and afadin deficiency in vivo.

Collectively, these data therefore support a model in which the transmembrane protein JAM-A is part of a complex containing afadin, ZO-1/2, and PDZ-GEF1 that induces activation of the small GTPase Rap2c and, through RhoA, controls contraction of the junction-associated apical cytoskeleton to maintain a functional and selectively permeable epithelial barrier. This model may provide new ideas for therapeutic targets that allow for the modulation of intestinal barrier function in health and disease.

MATERIALS AND METHODS

Cell culture

SK-CO15 human IECs were grown in DMEM supplemented with 10% fetal bovine serum, 2 mM L-glutamine, 100 IU of penicillin, 100 µg/ml streptomycin, 15 mM 4-(2-hydroxyethyl)-1-piperazineethanesulfonic acid (HEPES), and 1% nonessential amino acids and were subcultured with 0.05% trypsin (Cellgro, Manassas, VA). For filter-based studies, cells were seeded at a density of 1×10^5 cells/0.33 cm^2. Transfections were performed with Lipofectamine 2000 (Qiagen, Valencia, CA) in Optimem (Invitrogen, Carlsbad, CA) per manufacturer's protocol. Targets (Qiagen and Santa Cruz Biotechnology, Santa Cruz, CA; outlined in Supplemental Figure S4) were used at a total concentration of 100 nM siRNA or less, and knockdown was verified by Western blot or quantitative real-time PCR (qRT-PCR; Supplemental Figure S4). Cells were harvested for immunoblot, fixed for immunofluorescence staining, or assessed for barrier function 3 d after transfection.

Antibodies

The murine monoclonal anti–JAM-A antibodies 1H2A9, J10.4, and JF3.1 were purified as described (Liu *et al.*, 2000). Other antibodies were commercially available: polyclonal affinity-purified rabbit anti–JAM-A (Invitrogen); monoclonal mouse Rap2, monoclonal mouse anti–PDZ-GEF1, monoclonal mouse anti-afadin, monoclonal mouse ZO-1, and polyclonal affinity-purified rabbit ZO-2 (BD Transduction Laboratories, Lexington, KY); polyclonal affinity-purified rabbit anti–afadin 02246, monoclonal mouse anti-tubulin, and polyclonal affinity-purified rabbit anti-actin (Sigma-Aldrich, St. Louis, MO); polyclonal affinity-purified rabbit anti-Rap2c (Cell Signaling Technology, Beverly, MA); and polyclonal affinity-purified rabbit anti-RhoA (Santa Cruz Biotechnology). For immunoblots, horseradish peroxidase–conjugated secondary antibodies were used (Jackson ImmunoResearch Laboratories, West Grove, PA). For immunofluorescence, fluorescein isothiocyanate (FITC)- and Alexa-conjugated antibodies (Invitrogen) were used.

Expression and purification of the JAM-A–binding reovirus σ1 protein

A cDNA fragment encoding amino acids 170–455 of the σ1 attachment protein of reovirus strain T3D was fused to a GCN4-pII trimerization domain (www.biomers.net) and a 10–amino acid trypsin-cleavable linker. The resulting construct was inserted into a PQE-80L vector using *Bam*HI and *Hin*dIII sites. A G381A point mutant in σ1 was engineered using the GeneArt Site-Directed Mutagenesis System (Invitrogen) according to the manufacturer's protocol. Wild-type σ1 and σ1_G381A were expressed in DE3 *Escherichia coli* by autoinduction and purified as described previously (Reiter *et al.*, 2011).

Production of lentiviruses and stable cell lines

Lentiviruses were created in HEK293T TLA cells by transfection of viral plasmids (Open Biosystems, Huntsville, AL) with Lipofectamine 2000 (Qiagen). Lentivirus-containing media were harvested 72 h posttransfection. Titered supernates were then used at multiplicity of infection of 4 to transduce SK-CO15 human colonic epithelial cells. Resulting polyclonal populations were purified into different clones by serial dilutions and grown in supplemented DMEM with puromycin (2 µg/ml). Short hairpin RNA sequences are outlined in Supplemental Figure S4.

Immunoblots

Monolayers of epithelial cells were homogenized in radioimmunoprecipitation assay (RIPA) lysis buffer (20 mM Tris, 50 mM NaCl, 2 mM EDTA, 2 mM ethylene glycol tetraacetic acid, 1% sodium deoxycholate, 1% Triton X-100, and 0.1% SDS, pH 7.4) or 0.1% NP40 or 1% Brij 97 lysis buffer (10 mM Tris HCl, pH 8.0, 150 mM NaCl, 1 mM $MgCl_2$, 1 mM $CaCl_2$) supplemented with protease and phosphatase inhibitor cocktails (Sigma-Aldrich). A bicinchoninic acid assay (Pierce, Rockford, IL) was used to determine lysate protein concentrations. Lysates were cleared by centrifugation and boiled in reducing SDS sample buffer. SDS–PAGE and immunoblots were performed by standard methods. Tubulin was used as a protein loading control.

Immunoprecipitation

SK-CO15 and T84 cells that were 80–90% confluent were harvested in 0.1% NP40 or 1% Brij 97 lysis buffer supplemented with protease and phosphatase inhibitor cocktails (Sigma-Aldrich). Lysates were incubated end over end for 20 min at 4°C before being cleared at 14,000 rpm for 10 min. The supernatant (soluble fraction) was kept on ice while the pellet was resuspended in RIPA buffer, dounced, and cleared at 14,000 rpm for 10 min (RIPA fraction). Each fraction was precleared with 50 µl of Sepharose 4B for 30 min and incubated with 5 µg of antibody for 2 h. Immune complexes were precipitated by 50 µl of protein A– or protein G–Sepharose for 1 h. Immunoprecipitate pellets were washed three times in either lysis buffer or RIPA before being boiled in

reducing sample buffer. Input and immunoprecipitates were subjected to SDS–PAGE and immunoblotting.

Immunofluorescence microscopy

Cells were grown on 0.33-cm^2, 0.4-μm-pore Transwell filters (Corning Life Sciences, Lowell, MA), and human colonic tissue was flash frozen in OCT (Sakura, Alphen aan den Rijn, Netherlands) before being cryosectioned into 8-μm slices. Tissue and cells were pretreated for 5 min with 0.05% Triton X-100 in Hank's buffered saline solution (HBSS+; Cellgro) at room temperature or directly fixed in 100% ethanol at –20°C for 20 min and blocked in 5% bovine serum albumin in HBSS+ for 1 h. Samples to be characterized for cytoskeletal components were fixed in 3.7% Formalin for 10 min before being permeabilized with 0.1% Triton at room temperature or ethanol at –20°C. Primary antibodies were diluted in blocking buffer and incubated with cells overnight at 4°C. Fluorescently labeled secondary antibodies were diluted in blocking buffer and incubated with cells for 45 min at room temperature. Stained cells were washed in HBSS+ and mounted in Prolong Antifade Agent (Invitrogen). A laser scanning microscope (LSM 510; Carl Zeiss, Jena, Germany) was used to capture confocal fluorescence images. ImageJ (National Institutes of Health, Bethesda, MD) and LSM software (Carl Zeiss) were used for image processing.

PDZ-proteomic array

The PDZ domain–containing proteomic array has been previously described (Fam *et al.*, 2005; He *et al.*, 2006). Briefly, nylon membranes were spotted with recombinant His/S-tagged PDZ domain fusion proteins at a concentration of 1 μg/bin. GST fusion proteins corresponding to the C-terminal 25 amino acids of JAM-A, or a mutant with residues comprising the C-terminal PDZ binding motif (FLV) switched to alanines, were overlaid at concentrations of 100 nM in blotting buffer (2% nonfat dry milk, 0.1% Tween-20, 50 mM NaCl, 10 mM HEPES, pH 7.4) overnight at 4°C. Arrays were washed three times with blotting buffer, followed by incubation with horseradish peroxidase–conjugated anti-GST antibody (GE Healthcare, Piscataway, NJ). Interactions of GST fusion proteins and PDZ domains were visualized by chemiluminescence using an ECL Kit (Pierce)

RhoA and Rap2 activity assay

RhoA and Rap2 activity assays were performed according to the manufacturer's instructions (Millipore, Billerica, MA, and CellBio Labs, San Diego, CA). Briefly, cells were lysed at 4°C in a Tris and Triton X-100–based lysis buffer provided. Cell debris was removed by centrifugation and 40 μl saved as input to determine total RhoA or Rap2 level. Lysates containing equal amounts of protein for each sample (between 0.5 and 1.5 mg) were incubated at 4°C for 60 min with Rhotekin or Ral-GDS agarose beads to bind active RhoA (Reid *et al.*, 1996) or Rap2 (Knaus *et al.*, 2007), respectively. Beads were washed three times with lysis buffer, followed by boiling in SDS sample buffer. Entire samples were then analyzed by immunoblot with detection by RhoA or Rap2 antibody provided by the manufacturer.

Permeability assays

Cells were grown on 0.33-cm^2, 0.4-μm-pore Transwell filters (Corning Life Sciences) to confluence. TER to passive ion flow was recorded using an EVOMX voltmeter with an STX2 electrode (World Precision Instruments, Sarasota, FL). For dextran flux experiments, confluent monolayers grown on Transwell filters were washed and placed in HBSS+ (Invitrogen) for 1 h at 37°C. Rhodamine or FITC-conjugated dextran (3, 4, or 40 kDa; Sigma-Aldrich) was placed on the top chamber of Transwells for incubation for 2 h at 37°C. Samples from the bottom chamber of the Transwell were collected, and the fluorescence intensity was measured with a fluorescent plate reader (FLUOstar; BMG Labtech, Cary, NC).

In situ intestinal epithelial permeability was measured with a previously described intestinal loop model (Clayburgh *et al.*, 2005) with slight modifications. After overnight fasting, animals were anesthetized subcutaneously with a mixture of ketamine and xylazine at doses of 100 and 5 mg/kg, respectively. A midline abdominal incision was made to expose the small intestine, and a 4-cm loop was clipped at proximal and distal ends to isolate it from the rest of the bowel. For in vivo σ1 treatment studies, 100 μg/ml σ1 in HBSS+ was administered directly into the loop lumen for 1 h. Solutions containing FITC-dextran (3, 10, or 40 kDa; 1 mg/ml in HBSS) were then added to intestinal loops, and, after 1 h, fluorescence (an index of FITC-dextran absorption from the intestine lumen into the bloodstream) was measured from whole blood obtained by cardiac puncture, using a fluorescence microtiter plate reader (FLUOstar Galaxy; BMG LabTech). After cardiac puncture, all anesthetized mice were killed by cervical dislocation. All animal experiments were conducted according to protocols approved by the Institutional Animal Care and Use Committee at Emory University.

Fluorescence recovery after photobleaching

Stable NS or JAM-A–deficient (shJA) SK-CO15 cell lines were cultured on chamber slides (Thermo Fischer Scientific, Waltham, MA). At 50% confluence, cells were transduced with actin-GFP using a baculovirus delivery system (CellLight BacMam 2.0; Invitrogen). FRAP experiments were performed on a Nikon A1R TE 2000 inverted microscope (Nikon, Melville, NY) with a 40× objective, and GFP fluorescence was imaged with a 488-nm laser. All experiments were performed at 37°C with 5% CO_2 using a heating chamber. GFP fluorescence at cell contacts was bleached for 7 s using a 404-nm laser set at full power. To assess fluorescence recovery, images were acquired every 2 s over a period of 2 min. Fluorescence intensity data were corrected for overall loss in total fluorescence intensity as a result of fluorescence imaging and for loss of total cell fluorescence as a result of photobleaching. The fluorescence intensity of bleached regions over time was normalized to prebleached fluorescence intensity.

PCR and qRT-PCR

RNA was extracted from SK-CO15 cells with TRIzol (Invitrogen) and further purified with an RNA extraction kit (Qiagen). For standard PCR, RNA was subjected to reverse transcription (Invitrogen) and PCR using Taq Polymerase (Qiagen), and resulting DNA was assessed by agarose gel electrophoresis. qRT-PCR was performed with one-step SYBR Green (Bio-Rad, Hercules, CA). PCR and qRT-PCR were programmed as follows: 94°C for 3 min, followed by 40 cycles of 94°C for 15 s, 57°C for 30 s, and 72°C for 30 s. qRT-PCR data were represented as fold change, determined by applying the formula $2\Delta\Delta Ct$, where $\Delta Ct = Ct$ of target gene $- Ct$ of loading control (β-actin), and $\Delta\Delta Ct = \Delta Ct$ of samples for target gene (siRNA treated) $- \Delta Ct$ of the control for the target gene (scrambled siRNA treated). The primers used are outlined in Supplemental Figure S3.

Statistics

Statistical differences between target and scrambled siRNA–mediated knockdown groups were determined using a linear mixed effects modeling approach to control for random between-run differences in baseline TER while accurately measuring the effects of siRNA-mediated knockdown relative to controls. Results were scaled to a baseline of 100%, with 95% confidence intervals around the

effect. Statistically significant results indicate $p <$ type I error rate of 0.05. All statistical analyses were performed in the R statistical environment (R version 2.14; R Foundation for Statistical Computing, Vienna, Austria). For graphs representing three independent samples measured on the same day, a two-tailed Student's *t* test was used to determine *p* values between two experimental groups. $p < 0.05$ was considered significant.

ACKNOWLEDGMENTS

We thank Michael Koval, Christopher Capaldo, and Andrei Ivanov for useful comments and the Emory Cloning and DDRDC Cell Culture Cores for technical support. This work was supported by National Institutes of Health Grants DK061379, DK072564, and DK079392 (C.A.P.); DK59888 and DK55679 (A.N.); and DK064399 (C.A.P. and A.N.); a Crohn's and Colitis Foundation of America Career Development Award (R.S.); National Institutes of Health Grants R37AI38296, P30CA68485, and P60DK20593 (T.S.D.); Deutsche Forschungsgemeinschaft Grant KFO274 (T.S.); and National Institutes of Health Grant R01AI76983 (T.S. and T.S.D.).

REFERENCES

Altschul SF, Madden TL, Schäffer AA, Zhang J, Zhang Z, Miller W, Lipman DJ (1997). Gapped BLAST and PSI-BLAST: a new generation of protein database search programs. Nucleic Acids Res 25, 3389–3402.

Altschul SF, Wootton JC, Gertz EM, Agarwala R, Morgulis A, Schäffer AA, Yu Y-K (2005). Protein database searches using compositionally adjusted substitution matrices. FEBS J 272, 5101–5109.

Bazzoni G, Martínez-Estrada O, Orsenigo F, Cordenonsi M, Citi S, Dejana E (2000). Interaction of junctional adhesion molecule with the tight junction components ZO-1, cingulin, and occludin. J Biol Chem 275, 20520–20526.

Bruewer M, Hopkins AM, Hobert ME, Nusrat A, Madara JL (2004). RhoA, Rac1, and Cdc42 exert distinct effects on epithelial barrier via selective structural and biochemical modulation of junctional proteins and F-actin. Am J Physiol Cell Physiol 287, C327–C335.

Clayburgh DRD, Barrett TAT, Tang YY, Meddings JBJ, Van Eldik LJL, Watterson DMD, Clarke LLL, Mrsny RJR, Turner JRJ (2005). Epithelial myosin light chain kinase-dependent barrier dysfunction mediates T cell activation-induced diarrhea in vivo. J Clin Invest 115, 2702–2715.

Colegio OR, Van Itallie C, Rahner C, Anderson JM (2003). Claudin extracellular domains determine paracellular charge selectivity and resistance but not tight junction fibril architecture. Am J Physiol Cell Physiol C1346–C1354.

De Rooij J, Boenink NM, van Triest M, Cool RH, Wittinghofer A, Bos JL (1999). PDZ-GEF1, a guanine nucleotide exchange factor specific for Rap1 and Rap2. J Biol Chem 274, 38125–38130.

Ebnet K, Schulz C, Brickwedde MZ, Pendl GG, Vestweber D (2000). Junctional adhesion molecule interacts with the PDZ domain-containing proteins AF-6 and ZO-1. J Biol Chem 275, 27979–27988.

Fam SR, Paquet M, Castleberry AM, Oller H, Lee CJ, Traynelis SF, Smith Y, Yun CC, Hall RA (2005). P2Y1 receptor signaling is controlled by interaction with the PDZ scaffold NHERF-2. Proc Natl Acad Sci USA 102, 8042–8047.

Fanning AS, Jameson BJ, Jesaitis LA, Anderson JM (1998). The tight junction protein ZO-1 establishes a link between the transmembrane protein occludin and the actin cytoskeleton. J Biol Chem 273, 29745–29753.

Fanning AS, Van Itallie CM, Anderson JM (2012). Zonula occludens-1 and -2 regulate apical cell structure and the zonula adherens cytoskeleton in polarized epithelia. Mol Biol Cell 23, 577–590.

Furuse M (1998). Claudin-1 and -2: novel integral membrane proteins localizing at tight junctions with no sequence similarity to occludin. J Cell Biol 141, 1539–1550.

Furuse M (2010). Molecular basis of the core structure of tight junctions. Cold Spring Harb Perspect Biol 2, a002907–a002907.

Gloerich M, Klooster Ten JP, Vliem MJ, Koorman T, Zwartkruis FJ, Clevers H, Bos JL (2012). Rap2A links intestinal cell polarity to brush border formation. Nat Cell Biol 14, 793–801.

Guglielmi KM, Kirchner E, Holm GH, Stehle T, Dermody TS (2007). Reovirus binding determinants in junctional adhesion molecule-A. J Biol Chem 282, 17930–17940.

Gumbiner B, Lowenkopf T, Apatira D (1991). Identification of a 160-kDa polypeptide that binds to the tight junction protein ZO-1. Proc Natl Acad Sci USA 88, 3460–3464.

He J, Bellini M, Inuzuka H, Xu J, Xiong Y, Yang X, Castleberry AM, Hall RA (2006). Proteomic analysis of beta1-adrenergic receptor interactions with PDZ scaffold proteins. J Biol Chem 281, 2820–2827.

Hernandez S, Munguia BC, González-Mariscal L (2007). ZO-2 silencing in epithelial cells perturbs the gate and fence function of tight junctions and leads to an atypical monolayer architecture. Exp Cell Res 313, 15–15.

Hirase T, Kawashima S, Wong EYM, Ueyama T, Rikitake Y, Tsukita S, Yokoyama M, Staddon JM (2001). Regulation of tight junction permeability and occludin phosphorylation by RhoA-p160ROCK-dependent and -independent mechanisms. J Biol Chem 276, 10423–10431.

Iden S, Misselwitz S, Peddibhotla SSD, Tuncay H, Rehder D, Gerke V, Robenek H, Suzuki A, Ebnet K (2012). aPKC phosphorylates JAM-A at Ser285 to promote cell contact maturation and tight junction formation. J Cell Biol 196, 623–639.

Itoh M, Furuse M, Morita K, Kubota K, Saitou M, Tsukita S (1999). Direct binding of three tight junction-associated Maguks, ZO-1, ZO-2, and ZO-3, with the COOH termini of claudins. J Cell Biol 147, 1351–1363.

Ivanov AI, Bachar M, Babbin BA, Adelstein RS, Nusrat A, Parkos CA (2007). A unique role for nonmuscle myosin heavy chain IIA in regulation of epithelial apical junctions. PLoS One 2, e658.

Jou T-S, Schneeberger EE, Nelson WJ (1998). Structural and functional regulation of tight junctions by RhoA and Rac1 small GTPases. J Cell Biol 142, 101–115.

Khounlotham M *et al.* (2012). Compromised intestinal epithelial barrier induces adaptive immune compensation that protects from colitis. Immunity 37, 563–573.

Kirchner E, Guglielmi KM, Strauss HM, Dermody TS, Stehle T (2008). Structure of reovirus sigma1 in complex with its receptor junctional adhesion molecule-A. PLoS Pathog 4, e1000235.

Knaus UG, Bamberg A, Bokoch GM (2007). Rac and Rap GTPase activation assays. Methods Mol Biol 412 59–67.

Kooistra M, Dube N, Bos J (2007). Rap1: a key regulator in cell-cell junction formation. J Cell Sci 120, 17–22.

Kostrewa D, Brockhaus M, D'Arcy A, Dale G (2001). X-ray structure of junctional adhesion molecule: structural basis for homophilic adhesion via a novel dimerization motif. EMBO J 20, 4391–4398.

Kuiperij H, De Rooij J, Rehmann H, van Triest M, Wittinghofer A, Bos JL, Zwartkruis FJT (2003). Characterisation of PDZ-GEFs, a family of guanine nucleotide exchange factors specific for Rap1 and Rap2. Biochim Biophys Acta 1593, 141–149.

Laukoetter MG *et al.* (2007). JAM-A regulates permeability and inflammation in the intestine in vivo. J Exp Med 204, 3067–3076.

Liang TW *et al.* (2000). Characterization of huJAM: evidence for involvement in cell-cell contact and tight junction regulation. Am J Physiol Cell Physiol 279, C1733–C1743.

Liu Y, Nusrat A, Schnell FJ, Reaves TA, Walsh S, Pochet M, Parkos CA (2000). Human junction adhesion molecule regulates tight junction resealing in epithelia. J Cell Sci 113, 2363–2374.

Madara JL, Pappenheimer JR (1987). Structural basis for physiological regulation of paracellular pathways in intestinal epithelia. J Membrane Biol 100, 149–164.

Mandai K *et al.* (1997). Afadin: a novel actin filament-binding protein with one PDZ domain localized at cadherin-based cell-to-cell adherens junction. J Cell Biol 139, 517–528.

Mandell KJ, McCall IC, Parkos CA (2004). Involvement of the junctional adhesion molecule-1 (JAM1) homodimer interface in regulation of epithelial barrier function. J Biol Chem 279, 16254–16262.

McLeod SJ, Shum AJ, Lee RL, Takei F, Gold MR (2004). The Rap GTPases regulate integrin-mediated adhesion, cell spreading, actin polymerization, and Pyk2 tyrosine phosphorylation in B lymphocytes. J Biol Chem 279, 12009–12019.

Miyata M, Rikitake Y, Takahashi M, Nagamatsu Y, Yamauchi Y, Ogita H, Hirata K-I, Takai Y (2009). Regulation by afadin of cyclical activation and inactivation of Rap1, Rac1, and RhoA small G proteins at leading edges of moving NIH3T3 cells. J Biol Chem 284, 24595–24609.

Monteiro AC, Parkos CA (2012). Intracellular mediators of JAM-A-dependent epithelial barrier function. Ann NY Acad Sci 1257, 115–124.

Nava P *et al.* (2011). JAM-A regulates epithelial proliferation through Akt/β-catenin signalling. EMBO Rep 12, 314–320.

Nitta T, Hata M, Gotoh S, Seo Y, Sasaki H, Hashimoto N, Furuse M, Tsukita S (2003). Size-selective loosening of the blood-brain barrier in claudin-5–deficient mice. J Cell Biol 161, 653–660.

Noda K, Zhang J, Fukuhara S, Kunimoto S, Yoshimura M, Mochizuki N (2010). Vascular endothelial-cadherin stabilizes at cell-cell junctions by anchoring to circumferential actin bundles through alpha- and beta-catenins in cyclic AMP-Epac-Rap1 signal-activated endothelial cells. Mol Biol Cell 21, 584–596.

Nomme J, Fanning AS, Caffrey M, Lye MF, Anderson JM, Lavie A (2011). The Src homology 3 domain is required for junctional adhesion molecule binding to the third PDZ domain of the scaffolding protein ZO-1. J Biol Chem 286, 43352–43360.

Nusrat A, Giry M, Turner JR, Colgan SP, Parkos CA, Carnes D, Lemichez E, Boquet P, Madara JL (1995). Rho protein regulates tight junctions and perijunctional actin organization in polarized epithelia. Proc Natl Acad Sci USA 92, 10629–10633.

Nusrat A, Turner JR, Madara JL (2000). Molecular physiology and pathophysiology of tight junctions. IV. Regulation of tight junctions by extracellular stimuli: nutrients, cytokines, and immune cells. Am J Physiol Gastrointest Liver Physiol 279, G851–G857.

Pannekoek W-J *et al*. (2011). Epac1 and PDZ-GEF cooperate in Rap1 mediated endothelial junction control. Cell Signal 23, 2056–2064.

Prota AE, Campbell JA, Schelling P, Forrest JC, Peters TR, Aurrand-Lions M, Imhof BA, Dermody TS, Stehle T (2003). Crystal structure of human junctional adhesion molecule 1: implications for reovirus binding. Proc Natl Acad Sci USA 100, 5366–5371.

Reid T, Furuyashiki T, Ishizaki T, Watanabe G, Watanabe N, Fujisawa K, Morii N, Madaule P, Narumiya S (1996). Rhotekin, a new putative target for Rho bearing homology to a serine/threonine kinase, PKN, and Rhophilin in the Rho-binding domain. J Biol Chem 271, 13556–13560.

Reiter DM, Frierson JM, Halvorson EE, Kobayashi T, Dermody TS, Stehle T (2011). Crystal structure of reovirus attachment protein σ1 in complex with sialylated oligosaccharides. PLoS Pathog 7, e1002166.

Roscioni SS, Elzinga CRS, Schmidt M (2008). EPAC: effectors and biological functions. Naunyn Schmiedebergs Arch Pharmacol 377, 345–357.

Ryu J, Futai K, Feliu M, Weinberg R, Sheng M (2008). Constitutively active Rap2 transgenic mice display fewer dendritic spines, reduced extracellular signal-regulated kinase signaling, enhanced long-term depression, and impaired spatial learning and fear extinction. J Neurosci 28, 8178–8188.

Severson EA, Jiang L, Ivanov AI, Mandell KJ, Nusrat A, Parkos CA (2008). *Cis*-dimerization mediates function of junctional adhesion molecule A. Mol Biol Cell 19, 1862–1872.

Severson EA, Lee WY, Capaldo CT, Nusrat A, Parkos CA (2009). Junctional adhesion molecule A interacts with afadin and PDZ-GEF2 to activate Rap1A, regulate b1 integrin levels, and enhance cell migration. Mol Biol Cell 20, 1916–1925.

Shen L, Black E, Witkowski E, Lencer WI, Guerriero V, Schneeberger EE, Turner JR (2006). Myosin light chain phosphorylation regulates barrier function by remodeling tight junction structure. J Cell Sci 119, 2095–2106.

Shen L, Weber CR, Raleigh DR, Yu D, Turner JR (2011). Tight junction pore and leak pathways: a dynamic duo. Annu Rev Physiol 73, 283–309.

Takahashi K, Matsuo T, Katsube T, Ueda R, Yamamoto D (1998). Direct binding between two PDZ domain proteins Canoe and ZO-1 and their roles in regulation of the Jun N-terminal kinase pathway in *Drosophila* morphogenesis. Mech Dev 78, 97–111.

Tanaka-Okamoto M, Hori K, Ishizaki H, Itoh Y, Onishi S, Yonemura S, Takai Y, Miyoshi J (2011). Involvement of afadin in barrier function and homeostasis of mouse intestinal epithelia. J Cell Sci 124, 2231–2240.

Tsygankova O, Ma C, Tang W, Korch C, Meinkoth J (2010). Downregulation of Rap1GAP in human tumor cells alters cell/matrix and cell/cell adhesion. Mol Cell Biol 30, 3262–3274.

Van Itallie CM, Fanning AS, Anderson JM (2003). Reversal of charge selectivity in cation or anion-selective epithelial lines by expression of different claudins. Am J Physiol Renal Physiol 285, F1078–F1084.

Van Itallie CM, Fanning AS, Bridges A, Anderson JM (2009). ZO-1 stabilizes the tight junction solute barrier through coupling to the perijunctional cytoskeleton. Mol Biol Cell 20, 3930–3940.

Van Itallie CM, Rogan S, Yu A, Vidal LS, Holmes J, Anderson JM (2006). Two splice variants of claudin-10 in the kidney create paracellular pores with different ion selectivities. Am J Physiol Renal Physiol 291, F1288–F1299.

Yamazaki Y, Umeda K, Wada M, Nada S, Okada M, Tsukita S, Tsukita S (2008). ZO-1- and ZO-2-dependent integration of myosin-2 to epithelial zonula adherens. Mol Biol Cell 19, 3801–3811.

Zhang B, Lim TS, Vedula SRK, Li A, Lim CT, Tan VBC (2010). Investigation of the binding preference of reovirus sigma1 for junctional adhesion molecule A by classical and steered molecular dynamics. Biochemistry 49, 1776–1786.

Supplemental Materials

Molecular Biology of the Cell

Monteiro et al.

Supplemental Figures

Figure S1: Treatment of confluent T84 monolayers with σ1 for 3 hours led to significant reduction in TER when compared to cells treated with σ1_G381A mutant. Either WT σ1 or σ1_G381A (20 μg/ml) was added to apical and basolateral compartments. TER was evaluated at 1 and 3 hours (A, representative experiment with three independent samples. Bars represent mean +/- SD). SK-CO15 cells stably expressing non-silencing shRNA (NS) or shRNA targeting JAM-A (shJAM-A) were verified by immunoblot. SK-CO15 cells stably downregulated for JAM-A (shJAM-A) do not develop trans-epithelial resistance (TER) after four days of plating when compared to SK-CO15 cells stably expressing non-silencing shRNA (NS) (B, representative experiment with three independent samples. Bars represent mean +/- SD).

Figure S2: JAM-A (JA) co-immunoprecipitates with ZO-2 but not ZO-1 in intestinal epithelial cells. JAM-A immunoprecipitates from cell lysates prepared with a Triton X-100, Sodium deoxycholate and SDS based buffer (RIPA) revealed a 160 kDa ZO-2 immunoreactive band suggesting co-association between JAM-A and ZO-2, but did not reveal a 220 kDa ZO-1 immunoreactive band. Under the same conditions, ZO-2 immunoprecipitates revealed a 220 kDa ZO-1 immunoreactive band suggesting co-association between ZO-2 and ZO-1.

Figure S3: Sample qRT-PCR results verifying knockdown of targets in SK-CO15 cells used for in vitro permeability studies.

Figure S4: Additional PCR demonstrating lack of signal with alternate Rap2a primer pair. A common cDNA template and PCR master mix was prepared and then divided into four tubes containing specific primer pairs (A). Table outlining si/shRNA targets used in this study (B). Table outlining PCR primers used for PCR and qRT-PCR. Beta-actin was used as a housekeeping gene (C).

Figure S1

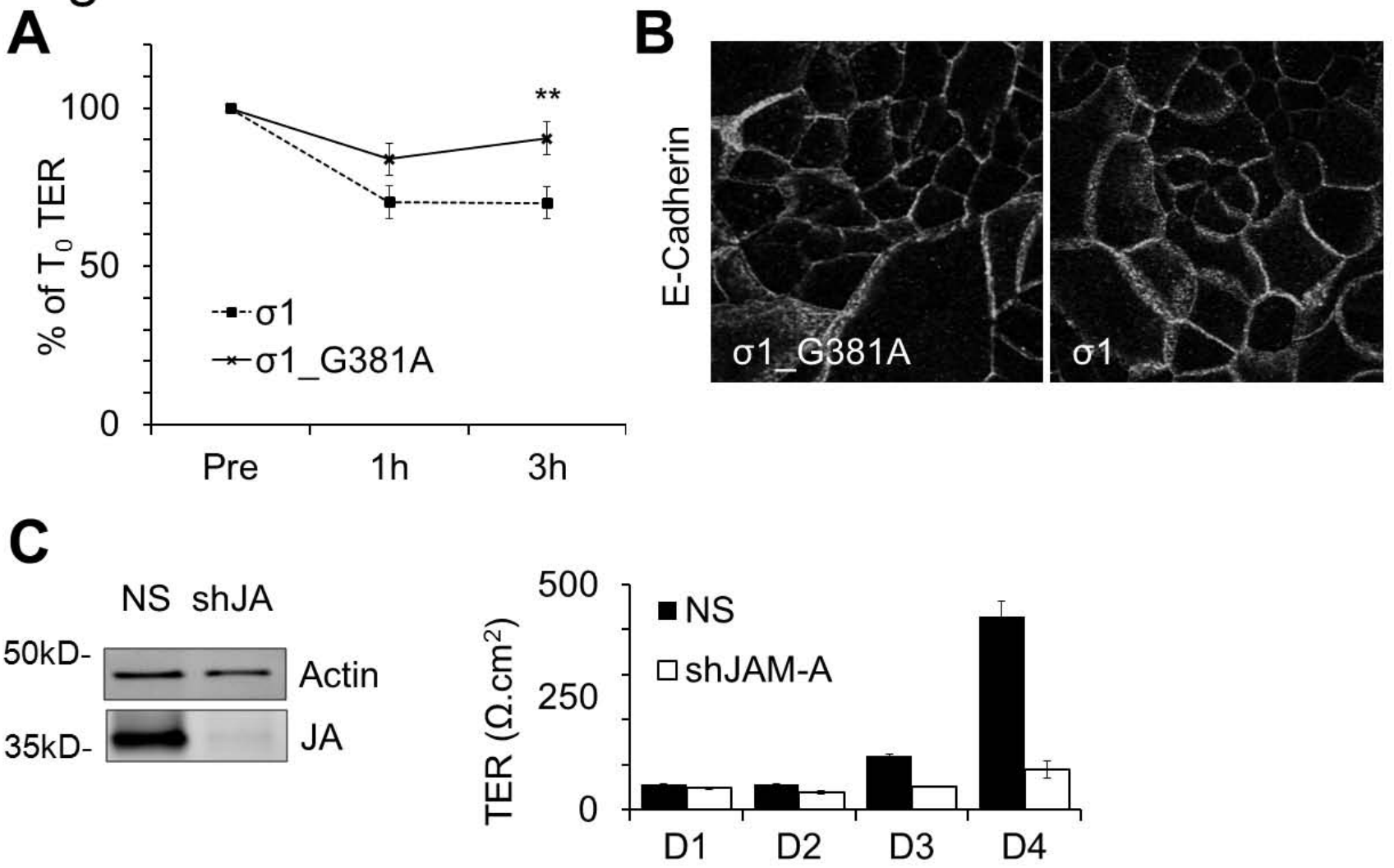
A
100
50
0
% of T0 TER
**
σ1
σ1_G381A
Pre
1h
3h
B
E-Cadherin
σ1_G381A
σ1
C
NS shJA
50kD-
Actin
35kD-
JA
500
250
0
TER (Ω.cm2)
NS
shJAM-A
D1
D2
D3
D4

Figure S2

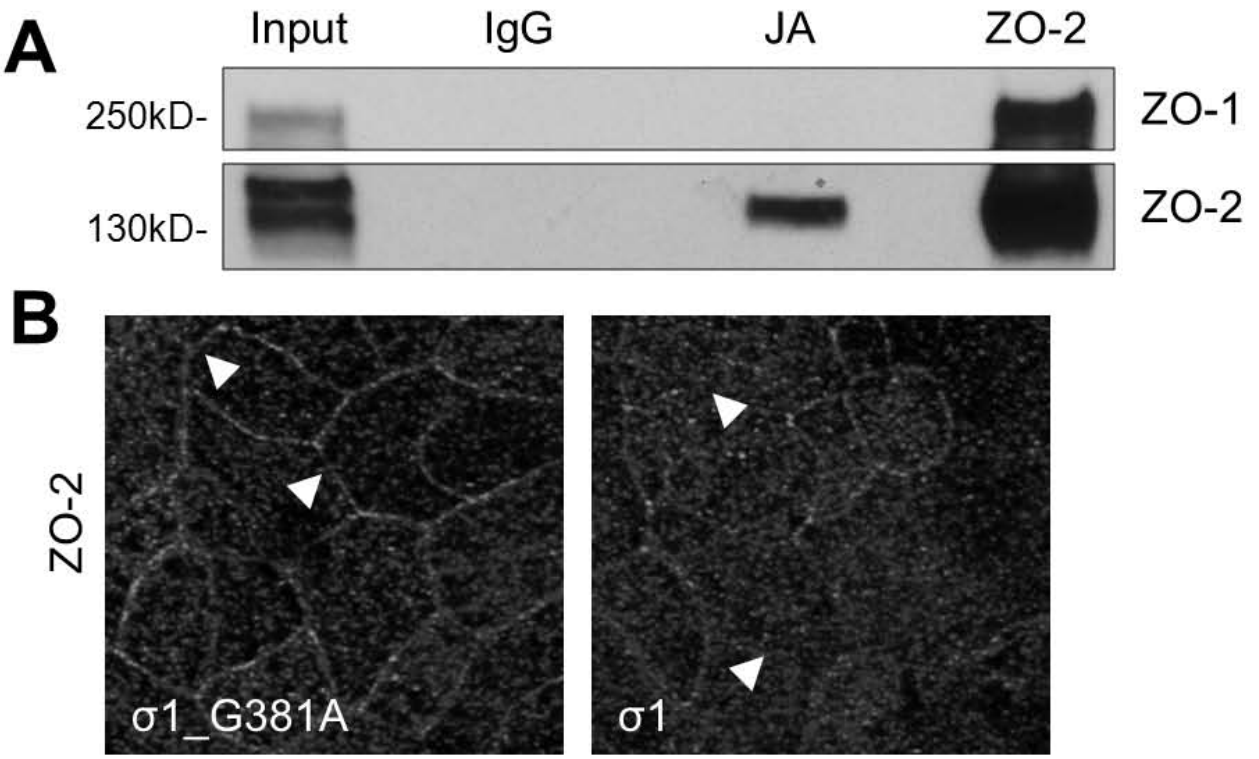

Figure S3

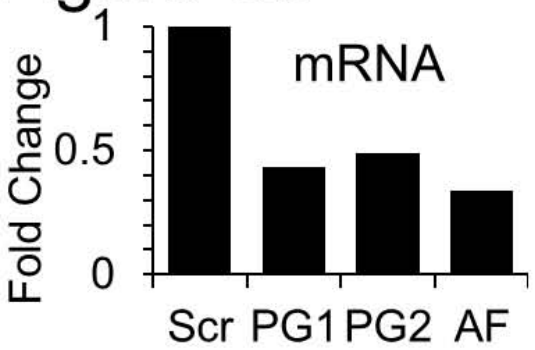
mRNA
Fold Change
1
0.5
0
Scr
PG1
PG2
AF

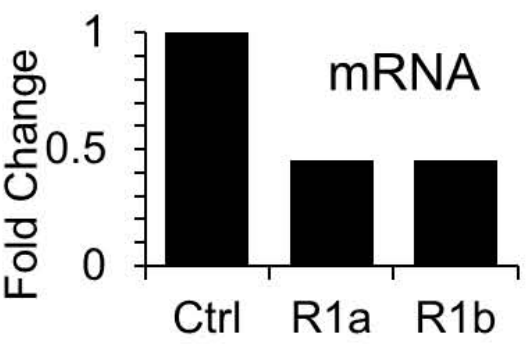
mRNA
Fold Change
1
0.5
0
Ctrl
R1a
R1b

Figure S4

A

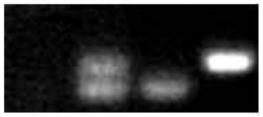

B

Target	si/shRNA sequences
Rap1A	5′-GAUCAAUGUUAAUGAGAUATT-3′
Rap1A'	5'-GCGAGUAGUUGGCAAAGAG-3'
Rap1B	5′-CGAGUACUGUGGAUGUGAATT-3′
Rap1B'	5'-GUAUAAUGUCUUAGAUUAATT-3'
Rap2B	5′-GGUGGUCUUAGUAAUAUAATT-3′
Rap2B'	5'-CACUUAAGUUUGAUAUCAATT-3'
Rap2C	5′-GGCUAAUAUACAAGGGUUATT-3′
Rap2C'	5'-UGUUCGUAUUAGAGACAAATT-3'
PDZ-GEF1	5′-GGAAGAAAGUGCCCGUAAATT-3′
PDZ-GEF1'	5′-CCGCUACAUCAUGAUCAGUAA-3′
PDZ-GEF2	5'-CUGCAUGAAUUGUAACUGAA3'
PDZ-GEF2'	CAGGAAGAAGGGACAAACAAA
Afadin	5'-UGAGAAACCUCUAGUUGUA-3'
Afadin'	5'-GUUAAGGGCCCAAGACAUA-3'
JAM-A	5'-GAAGUGAAGGAGAAUUCAATT-3'
JAM-A'	5'-CGGGUGACCUUCUUGCCAATT-3'
Scramble	Proprietary (Qiagen, USA)
shNS	5'-GGAATCTCATTCGATGCATAC-3'
shJAM-A	5'-TGAGAATAATCCTGTGAAGTT-3'
shJAM-A'	5'-ACAACAGGAGAGCTGGTCTTT-3'

C

Target	Forward Primer	Reverse Primer
Rap1A	5′-GGCAAAGAGCAGGGCCAGAATT-3′	5′-CTAGAGCAGCAGACATGATTTC-3′
Rap1B	5′-GGGAAGGAACAAGGTCAAAATC-3′	5′-TTAAAGCAGCTGACATGATG-3′
Rap2A	5′-CATGCTGTTCTGCATGTAAC-3′	5′-CAAGTTCTGCAGTGGAGTAG-3′
Rap2A'	5'-TCCGCGTGAAGCGGTATGAGA-3'	5'-AGGGCTCTGCCTTCGCTGCA-3'
Rap2B	5′-GGCCCTGGCTGAGGAGTGGA-3′	5′-GAGGATCACGCAGGCCGAGC-3′
Rap2C	5'-TGGCCATACCGAGCAGATAAAACTCA-3'	5'-ACAGGTTTACCAAGGCTCAGTTCTGC-3'
PDZ-GEF1	5′-AAATTCGTCACGTTGGCCGAATGG-3′	5′-ACTCCGCCATTTCTTCTTCCGAGT-3′
PDZ-GEF2	5′-TGTTGACTCCATGTCTGCAGCTCT-3′	5′-ACCCAGGGCCATGTTGACTATGAT-3′
Afadin	5'-CCGACATCATCCACCACTGG-3'	5'-CAGCATTCGCATATCAGGTCG-3'
JAM-A	5'-GTTGTCCTGTGCCTACTCGG-3'	5'-CCGTGTCACGGACTTGAAGG-3'
Beta-Actin	5'-TGACCCAGATCATGTTTGAGA-3'	5'-AGTCCATCACGATGCCAGT-3'